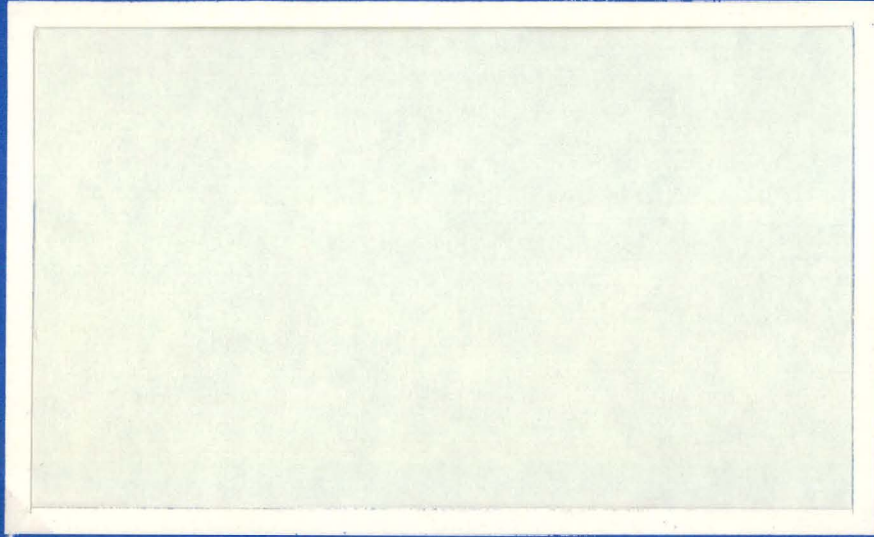


204
12-21

1656

MASTER



WADCO
CORPORATION

a subsidiary of Westinghouse Electric Corporation
Post Office Box 1970
Richland, Washington 99352

DISTRIBUTION OF THIS DOCUMENT IS UNLIMITED

P7876

DISCLAIMER

This report was prepared as an account of work sponsored by an agency of the United States Government. Neither the United States Government nor any agency Thereof, nor any of their employees, makes any warranty, express or implied, or assumes any legal liability or responsibility for the accuracy, completeness, or usefulness of any information, apparatus, product, or process disclosed, or represents that its use would not infringe privately owned rights. Reference herein to any specific commercial product, process, or service by trade name, trademark, manufacturer, or otherwise does not necessarily constitute or imply its endorsement, recommendation, or favoring by the United States Government or any agency thereof. The views and opinions of authors expressed herein do not necessarily state or reflect those of the United States Government or any agency thereof.

DISCLAIMER

Portions of this document may be illegible in electronic image products. Images are produced from the best available original document.

[REDACTED] LEGAL NOTICE

This report was prepared as an account of work sponsored by the United States Government. Neither the United States nor the United States Atomic Energy Commission, nor any of their employees, nor any of their contractors, subcontractors, or their employees, makes any warranty, express or implied, or assumes any legal liability or responsibility for the accuracy, completeness or usefulness of any information, apparatus, product or process disclosed, or represents that its use would not infringe privately owned rights.

HANFORD ENGINEERING DEVELOPMENT LABORATORY

Richland, Washington
operated by

WADCO CORPORATION

A Subsidiary of Westinghouse Electric Corporation
for the

United States Atomic Energy Commission Under Contract No. AT(45-1)-2170

UC-25, Metals,
Ceramics, and
Materials

EVALUATION OF PuO_2 HOMOGENEITY
IN $\text{PuO}_2\text{-UO}_2$ FAST REACTOR FUEL
BY SCANNING ELECTRON MICROPROBE

D. A. Stranik
H. G. Powers
G. A. Last

THIS DOCUMENT CONFIRMED AS
UNCLASSIFIED
DIVISION OF CLASSIFICATION
BY 911/Calvin J. Amb
DATE 12/31/70

October, 1970

FIRST UNRESTRICTED
DISTRIBUTION MADE

DEC 07 '70



LEGAL NOTICE

This report was prepared as an account of work sponsored by the United States Government. Neither the United States nor the United States Atomic Energy Commission, nor any of their employees, nor any of their contractors, subcontractors, or their employees, makes any warranty, express or implied, or assumes any legal liability or responsibility for the accuracy, completeness or usefulness of any information, apparatus, product or process disclosed, or represents that its use would not infringe privately owned rights.

UNCLASSIFIED

DISTRIBUTION OF THIS DOCUMENT IS UNLIMITED

leg

24 KENNERICK DOCUMENTS ARE
PROVIDED
BY
DIVISION OF THE
DATA

Printed in the United States of America
Available from
National Technical Information Service
National Bureau of Standards, U.S. Department of Commerce
Springfield, Virginia 22151
Price: Printed Copy \$3.00; Microfiche \$0.65

EVALUATION OF PuO_2 HOMOGENEITY IN $\text{PuO}_2\text{-UO}_2$ FAST REACTOR FUEL
BY SCANNING ELECTRON MICROPROBE

D. A. Stranik
H. G. Powers
G. A. Last

ABSTRACT

Quantitative characterization of a $(\text{Pu}_{0.25}\text{U}_{0.75})\text{O}_2$ fuel pellet matrix was accomplished by scanning pellets with an electron microprobe for PuO_2 concentration sizes of PuO_2 enriched or depleted zones and separation distance of such zones. Statistical analyses of the data indicated less than 1 percent probability of occurrence of zones with peak PuO_2 concentration greater than 50 wt% and less than 1 percent probability of occurrence of PuO_2 enriched or depleted zones having diameters greater than 50 microns. This technique enabled a mathematical model to be developed relating fuel pellet characteristics to a figure of merit which describes the homogeneity of mixed oxide fuel in terms of the degree of uniformity of energy deposition (or temperature rise) under reactor transient conditions in the UO_2 content of the fuel. By definition, the local figure of merit, M , at any point in the fuel is equal to the ratio of the local rate of deposition of energy as compared to that which would exist in a homogeneous fuel of average composition. Since the model used in the development of the figure of merit does not allow for diffusion of energy, the figure of merit represents the limiting thermal response of mixed oxide fuel under transient conditions. The model defines a term (D_x) as the product of the calculated local heat generation rate and local UO_2 concentration.

$$D_x = \left[K_3 \overline{C_{PuO_2}}_x + K_4 \overline{1-C_{PuO_2}}_x \right] C_{UO_2}_x$$

using $K_3 = \frac{1.9^*}{1.9 + 0.05}$ and $K_4 = \frac{0.05^*}{1.9 + 0.05}$

$$D_x = \left(0.026 + 0.948 \overline{C_{PuO_2}}_x \right) \left(\overline{1-C_{PuO_2}}_x \right)$$

$$M_x = \frac{D_x}{\overline{D}_x}$$

where \overline{D}_x is that calculated for a homogeneous fuel.

A test was designed to verify the model and to determine the homogeneity of pellets with a wide range of homogeneities based upon previous alpha-autoradiographs. The powder preparation varied for the four pellets. Results of the test indicated that the approach was feasible.

In order for industry to use this model to establish homogeneity in the fuel for the FFTF, it was determined that the correlation between figure of merit and alpha-autoradiography would be developed. This would permit the utilization of a relatively inexpensive and simple test method. Standards were made having a range of figures of merit which were then alpha-autoradiographed. These standards of known homogeneity are compared to pellets with unknown homogeneity by using alpha-autoradiographs taken at the same time. From this visual comparison with the standards, a figure of merit for the unknown pellets can be determined. This method of relating the figure of merit to alpha-autoradiography makes the homogeneity specification feasible for industrial measurement and use.

CONTENTS

LIST OF FIGURES	vii
INTRODUCTION	1
SUMMARY	2
DESIGN OF TESTS	3
DISCUSSION	4
Experimental Procedure	4
Experimental Results	6
Homogeneity Model	9
Experimental Results of Model	14
Application of Homogeneity Model	20
CONCLUSIONS	20
ACKNOWLEDGMENTS	23
REFERENCES	24
APPENDIX	A-1

THIS PAGE
WAS INTENTIONALLY
LEFT BLANK

LIST OF FIGURES

1. Probability of Fuel Distribution Within Pellet	8
2. Variation of \bar{D}_x with Plutonium Concentration in UO_2-PuO_2 Fuel Pellets	13
3. Hypothetical Distribution Curve for Figure of Merit M_x in a Heterogeneous UO_2-PuO_2 Fuel Pellet	14
4. Plutonium Concentration for Theoretic 20 Micron Sphere	15
5. Homogeneity Results	16
6. Figure of Merit Distribution for Pellet 1	17
7. Figure of Merit Distribution for Pellet 2	18
8. Figure of Merit Distribution for Pellet 3	19
9. Figure of Merit Distribution for Pellet 4	19
10. Determination of Fuel Pellet Homogeneity Using Figure of Merit Reference Pellets	21

EVALUATION OF PuO_2 HOMOGENEITY IN $\text{PuO}_2\text{-UO}_2$ FAST REACTOR FUEL
BY SCANNING ELECTRON MICROPROBE

D. A. Stranik
H. G. Powers
G. A. Last

INTRODUCTION

Evaluation of the effect of variations of concentration within a mixed oxide fuel pellet on the Doppler coefficient and thermal performance requires knowledge of the sizes of plutonium enriched areas, plutonium concentrations and inter-area distances.

The purpose of this report is to provide the theory and the experimental data for measuring homogeneity of fuel pellets based on the functional performance requirements of the fuel in the reactor. The functional performance is the thermal response of the mixed oxide fuel under transient conditions.

Assessment of process capabilities for controlling fuel pellet homogeneity has been limited in the past by the lack of an accurate quantitative measurement method. The volume, the average concentration of plutonium in enriched or depleted zones, and interzone distances have an important effect on performance of the fuel pellet; therefore, these features should be determined by the measurement method. The alpha-autoradiography technique at its present stage of development does not provide the desired accuracy in determining the size of enriched or depleted zones, and provides no quantitative data concerning PuO_2 concentration of such zones.

SUMMARY

A method for quantitative measurement of fuel pellet homogeneity has been developed which in turn has permitted the development of an improved homogeneity specification.

Quantitative characterization of the fuel pellet matrix was accomplished by scanning the pellets with the electron microprobe for PuO_2 concentration, sizes of PuO_2 enriched or depleted zones, and separation distance of such zones.

Pellets from 23 sintered batches of fuel were sampled and analyzed. The $(\text{Pu}_{0.25}\text{U}_{0.75})\text{O}_2$ fuel pellets were fabricated from mechanically blended mixed oxides by ballmilling, pressing, and sintering. Three pellets from each batch were sectioned and scanned using the microprobe. Two were mounted as transverse sections and one as a longitudinal section. The pellets were 0.212 inch in diameter and 0.250 inch in length.

The microprobe data were used in establishing an additional homogeneity model based upon an oxide matrix representative of typical production control capabilities and including the effects of localized heating due to zones of varying size, enrichment, and segregation.

Statistical analyses of the data indicate less than 1 percent probability of occurrence of zones with peak PuO_2 concentrations greater than 50 wt% and less than 1 percent probability of occurrence of enriched or depleted PuO_2 zones having diameters greater than 50 microns.

This mathematical model relates fuel pellet characteristics to a figure of merit which describes the homogeneity of mixed oxide fuel in terms of the degree of uniformity of energy deposition (or temperature rise) under transient conditions in the UO_2 content of the fuel. By definition, the local figure of merit, M , at any point in the fuel is equal to the ratio of the local rate of energy deposition at that point as compared

to that which would exist in a homogeneous fuel of average composition. Since the model used in the development of the figure of merit does not allow for diffusion of energy, the figure of merit represents the limiting thermal response of $UO_2 + PuO_2$ fuel under transient conditions. A mean value of M of 0.9 was established as meeting FTR requirements.

Microprobe data from three $(Pu_{0.25}U_{0.75})O_2$ fuel pellets with three different degrees of homogeneity were analyzed to test the model. The powder preparation was varied for the four pellets; Pellet 1 was wet ballmilled ~16 hours, Pellet 2 was dry ballmilled ~40, Pellet 3 was dry ballmilled ~20, and Pellet 4 was dry ballmilled ~10 hours. Results of the test indicate that the four pellets were greater than $\bar{M} = 0.95$.

DESIGN OF TESTS

Two tests were designed in order to derive the homogeneity model. The first test was designed to determine quantitatively by use of the scanning electron microprobe PuO_2 concentrations, sizes of PuO_2 enriched or depleted zones and the frequency of occurrence. The pellets were irradiation test pellets taken from 23 sintering batches. From the data, a theoretical homogeneity model was established based on heat generation rates and energy disposition within the UO_2 - PuO_2 pellets. A second test was designed to verify the model and to determine the homogeneity of several pellets with a wide range of homogeneities based on alpha-autoradiographs.

DISCUSSION

EXPERIMENTAL PROCEDURE

Pellets from 23 sintering batches were selected at random for electron microprobe analyses. The $(Pu_{0.25}U_{0.75})O_2$

fuel pellets were fabricated from mechanically blended mixed oxides, ballmilling, binder addition, pressing, and sintering. Three pellets from each batch were sectioned, polished, and scanned using the microprobe. Two pellets from each sintering batch were mounted as transverse sections and one as a longitudinal section. The pellets were approximately 0.212 inch in diameter and 0.250 inch in length.

The microprobe measurements were obtained using a 1 micron beam diameter and a scanning speed sufficiently slow to eliminate errors due to instrument response time. The narrow beam was used in order to reduce the averaging effect of larger size beams and to better resolve concentration gradients.

The intensity of characteristic X-rays of plutonium and uranium was measured and related quantitatively to percent PuO_2 and UO_2 in the volume of material excited by the electron beam. This volume is in the order of 1 to 1.5 cubic microns.

An electron microprobe, MAC Model 400 S/N 110 was used having three X-ray spectrometers with separate counting channels. The focusing crystals measured X-rays with wave lengths in the 3.4 to 4.2 angstrom range.

A simultaneous reading of peak and background X-ray counts were recorded for plutonium and uranium X-ray. This was done by reading the background on a third spectrometer and relating this background to the background of plutonium and uranium X-rays on the other spectrometers. The relationship of the third spectrometer background reading 4.1583 angstroms to Spectrometer 1 and 2 was as follows:

$$\text{Background Spectrometer 1} = 3.5 + 0.345 \text{ (Spectrometer 3)}$$

$$\text{Background Spectrometer 2} = 3.5 + 0.827 \text{ (Spectrometer 3).}$$

These equations were found by plotting the average plutonium background and average uranium background versus Spectrometer 3 background for various specimen current on a $\text{PuO}_2\text{-UO}_2$ pellet. The average plutonium background was found by averaging readings at 1.270 and 1.370 on a LiF calibrated scale using an ADP crystal. The average uranium background was found by averaging readings at 1.450 and 1.520 on a LiF calibrated scale using an ADP crystal. The X-ray intensity from the third spectrometer was measured at a setting of 1.916 on a LiF calibrated scale using a PET crystal. A minimum of five sets of X-ray intensity readings were measured at any one specimen current setting. Five different specimen current settings were used. The detector high voltage was changed for one of the channels to achieve linearity.

The uranium $M\alpha$ (3.924 angstroms) was measured on Spectrometer 1, plutonium $M\beta$ (3.515 angstroms) on Spectrometer 2, and the background on the third spectrometer.

An accelerating voltage in the range of 15 to 30 kV was used. Interference from high order L lines was eliminated by pulse height analysis.

The relationship of plutonium and uranium concentration to the measured relative M line intensities was found to be linear with no correction needed for absorption, fluorescence, or atomic number. Other investigators have also found this linearity. (1,2)

For the 10 second counting duration there is a 95 percent confidence that 95 percent of the measured X-ray intensities for a 25 wt% sample will be between the following limits, assuming a purely homogeneous matrix:

<u>Counts/sec</u>	<u>wt%</u>
1000	24.50 to 25.50
2000	24.65 to 25.35
4000	24.75 to 25.25

The results of the scans were printed out on charts for analyses. The data were obtained from the charts by recording the PuO_2 concentration and size of each indicated enriched or plutonium depleted zone.

EXPERIMENTAL RESULTS

Pellets from 23 sintered batches of fuel were sampled and analyzed. The $(\text{Pu}_{0.25}\text{U}_{0.75})\text{O}_2$ fuel pellets were fabricated from mechanically blended mixed oxides by ball-milling, pressing, and sintering. Three pellets from each batch were sectioned and scanned using the microprobe. Two were mounted as transverse sections and one as a longitudinal section. The pellets were 0.212 inches in diameter and 0.250 inches in length.

The data printed on strip charts were analyzed by determining the concentration of plutonium enriched zones within the pellet, the size of the PuO_2 enriched or depleted zones at the matrix composition of 25 wt%, and the separation distance of such zones.

The mathematical model for the three-dimensional graph of weight percent PuO_2 , width of peak at 25 percent PuO_2 and frequency of occurrence showing the probability of PuO_2 distribution within a pellet is given below: Let the two-dimensional random variable (x,y) have the joint density

$$f(x,y) = \frac{1}{2\pi \sigma_x \sigma_y \sqrt{1-\rho^2}} e^{-\frac{1}{2(1-\rho^2)} \left(\frac{(x-\mu_x)^2}{\sigma_x^2} - 2\rho \left(\frac{x-\mu_x}{\sigma_x} \right) \left(\frac{y-\mu_y}{\sigma_y} \right) + \frac{(y-\mu_y)^2}{\sigma_y^2} \right)}$$

$-\infty < x < \infty,$
 $-\infty < y < \infty,$

where σ_x , σ_y , μ_x , μ_y , ρ are constants such that

$$-1 < \rho < 1, \quad -\infty < \mu_x < \infty,$$

$$0 < \sigma_x,$$

$$0 < \sigma_y, \quad -\infty < \mu_y < \infty,$$

Then the random variable is said to have a bivariate normal distribution.

The bivariate normal distribution of interest is the one for the following two variables:

$$x = \log_e (\text{width of peak at 25 percent concentration})$$

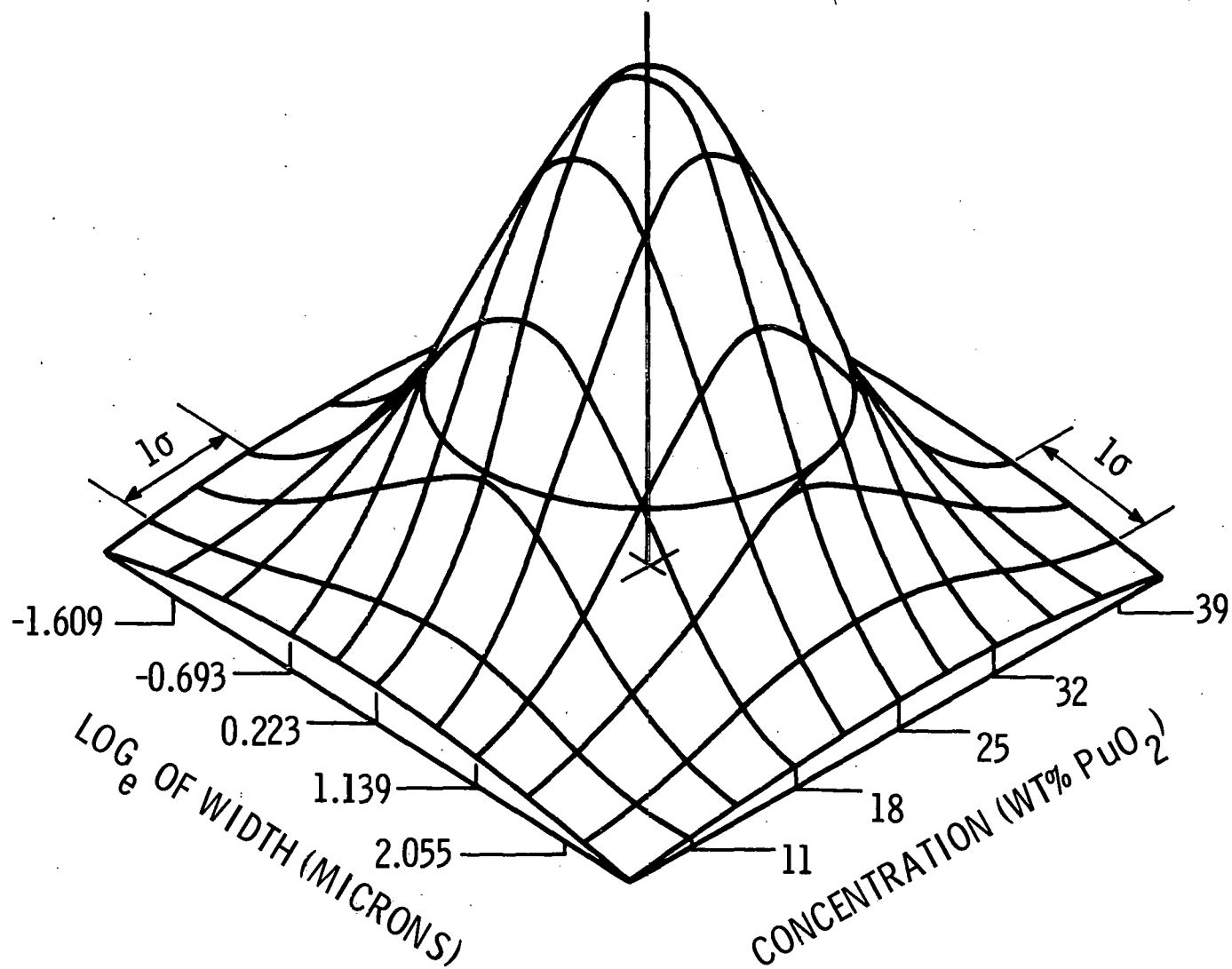
$$y = \text{wt\% concentration}$$

Estimates for the constants were obtained from the analysis of microprobe measurements made on ten samples from a series of 23 sintering batches of fuel pellets with 25 wt% PuO_2 concentration. The estimates are:

$$\hat{\mu}_x = 0.223 \quad \hat{\sigma}_x = 0.916 \quad \hat{\rho} = -0.0632$$

$$\hat{\mu}_y = 25.0 \quad \hat{\sigma}_y = 7.0$$

The shape of this three dimensional graph is shown in Figure 1.



Neg 703054-1

FIGURE 1. Probability of Fuel Distribution Within Pellet

WHAN-FR-20

Statistical analyses of the data indicate less than 1 percent probability of occurrence of zones with peak PuO_2 concentrations greater than 50 wt%. They show less than 1 percent probability of occurrence of enriched or depleted zones having diameters greater than 50 microns. Thus, the fuel was acceptable 99% of the time using a 50 micron particle size specification.

As a result of this work it was determined that a quantitative analysis of the fuel relating to the functional performance of the fuel within the reactor could be obtained. Thus, a mathematical model was developed describing the homogeneity of the mixed oxide fuel as a function of energy deposition within the fuel.

HOMOGENEITY MODEL

The mathematical model developed relates fuel pellet characteristics to a figure of merit. The figure of merit describes the homogeneity of mixed oxide fuel in terms of the degree of uniformity of energy deposition (or temperature rise) under transient conditions in the UO_2 content of the fuel. By definition, (the local figure of merit, M , at any point in the fuel is equal to the calculated relative rate of energy deposition at that point divided by the deposition rate which would exist in a homogeneous fuel of average composition). Since the model used in the development of the figure of merit does not allow for diffusion of energy, the figure of merit represents the limiting thermal response of mixed oxide fuel under transient conditions. The model defines a term (D_x) as the product of the calculated local heat generation rate and local UO_2 concentration. A figure of merit (M) is obtained by dividing D_x by an equivalent term \overline{D}_x which is calculated for a theoretically homogeneous fuel.

$$D_x \text{ is defined as: } D_x = K_1 \times E_x \times C_{UO_2} \quad (1)$$

where

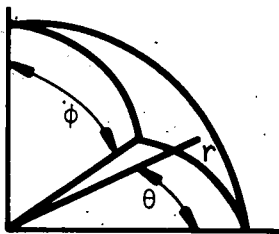
E_x = energy deposition rate at point x

The rate of temperature rise at point x is assumed to be directly proportional to E_x ; i.e., the heat capacity of the fuel is constant.

Equation (1) can be rewritten:

$$D_x = K_1 \cdot K_2 \cdot \overline{FP}_x \cdot C_{UO_2} \quad (2)$$

Calculation of FP for UO_2 - PuO_2 Fuel



$$d \overline{FP}_x = \frac{K_3 C_{PuO_2} (r, \theta, \phi) + K_4 C_{UO_2} (r, \theta, \phi) \cdot r^2 \sin \phi dr d\theta d\phi}{4 \pi r^2}$$

where K_3 and K_4 are constants proportional to the fission cross section of uranium and plutonium, or

$$d \overline{FP}_x = \left[K_3 \overline{C_{PuO_2}}(r) + K_4 (1 - \overline{C_{PuO_2}})(r) \right] dr \quad (3)$$

where $\overline{C_{PuO_2}}(r)$ is the average PuO_2 content at radius r.

On the basis the fission product track length is 10 microns and energy deposition is uniform along the track and integrating Equation 3 between $r = 0$ and $r = +10$ microns

$$\overline{FP}_x = K_3 \overline{C_{PuO_2}}_x + K_4 \left(1 - \overline{C_{PuO_2}}_x \right) \quad (4)$$

where $\overline{C_{PuO_2}}_x$ = average PuO_2 content along a diameter of a 20 micron sphere centered at point x.

Substituting Equation (4) in (2)

$$D_x = \left[K_3 \overline{C_{PuO_2}}_x + K_4 \left(1 - \overline{C_{PuO_2}}_x \right) \right] C_{UO_2}_x$$

using $K_3 = \frac{1.9*}{1.9+0.05}$ and $K_4 = \frac{0.05*}{1.9+0.05}$

$$D_x = \left[0.974 \overline{C_{PuO_2}}_x + 0.026 \left(1 - \overline{C_{PuO_2}}_x \right) \right] C_{UO_2}_x \quad (5)$$

$$D_x = \left(0.026 + 0.948 \overline{C_{PuO_2}}_x \right) \left(1 - \overline{C_{PuO_2}}_x \right)$$

where $\overline{C_{PuO_2}}_x$ = average PuO_2 content along a diameter of a 20 micron sphere centered at point x.

Thus, for homogeneous fuel,

$$\overline{D}_x = \left(0.026 + 0.948 \overline{\overline{C_{PuO_2}}} \right) \left(1 - \overline{\overline{C_{PuO_2}}} \right) \quad (6)$$

where $\overline{\overline{C_{PuO_2}}}$ is the PuO_2 content of the homogeneous mixed oxide fuel.

* Effective fission cross sections for fissile and fertile atoms in FFTF.

The relationship between $\overline{C_{PuO_2}}$ and $\overline{D_x}$ is shown in Figure 2.

By definition,

$$M_x = \frac{D_x}{\overline{D_x}} \quad (7)$$

where M is the local figure of merit at point x and

$$\bar{M} = \frac{1}{N} \sum \frac{D_x}{\overline{D_x}} \quad (8)$$

where \bar{M} is the average figure of merit for N determinations.

The value of $\overline{C_{PuO_2}}$ calculated for any point x on the microprobe trace will be conservative in terms of using Equation (2) to establish a distribution curve for D_x values since the "observed" value of $\overline{C_{PuO_2}}$ will statistically vary about the true mean value of $\overline{C_{PuO_2}}$ for a hypothetical 20 micron diameter sphere centered at point x .

This statistical variation will result in an increased spread in the calculated M_x values used to establish a distribution curve

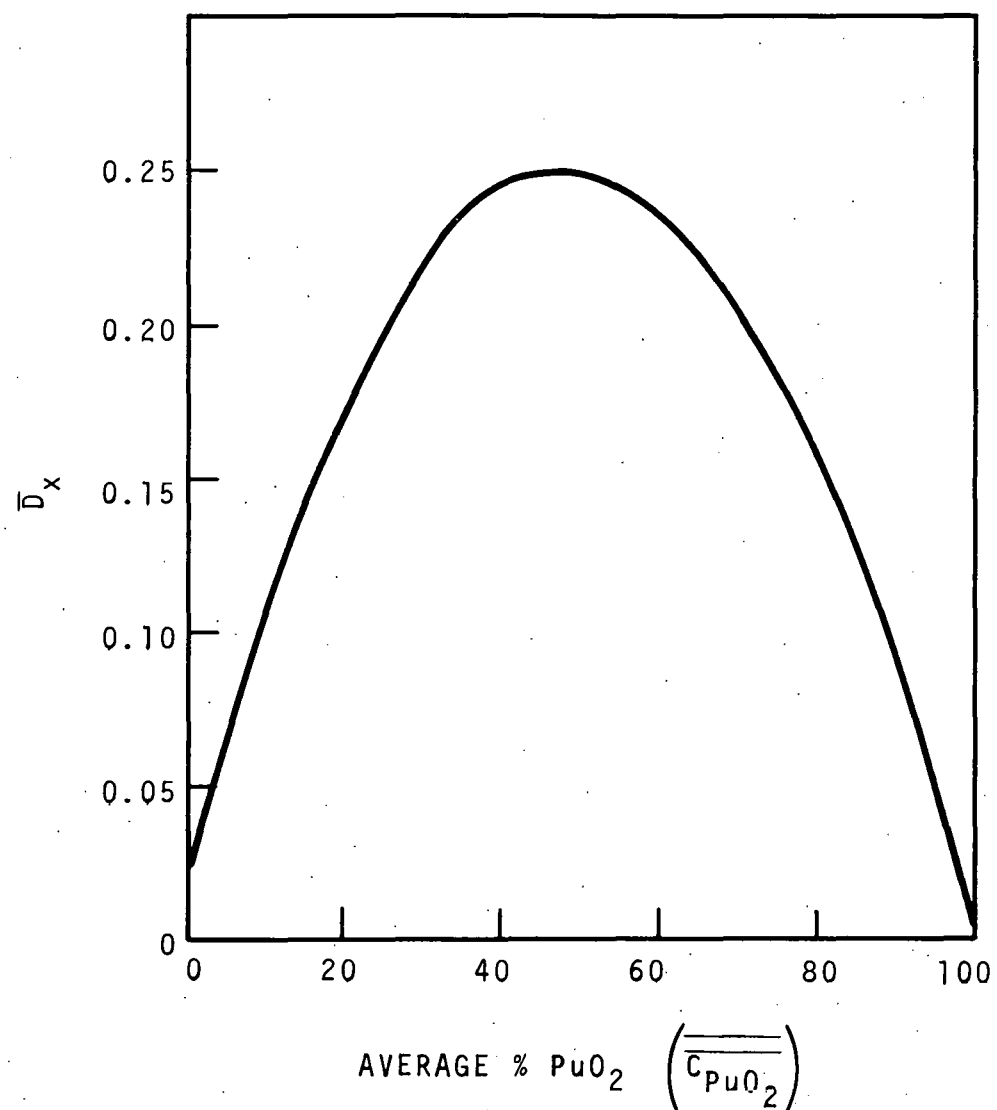


FIGURE 2. Variation of \overline{D}_x with Plutonium Concentration in UO_2-PuO_2 Fuel Pellets

Figure 3 illustrates the type of M_x distribution curve to be expected from a heterogeneous pellet. Two properties of the curve can be used to describe homogeneity requirements: (1) the value of M , and (2) the fraction of M_x values which falls within a specified limit about \bar{M} .

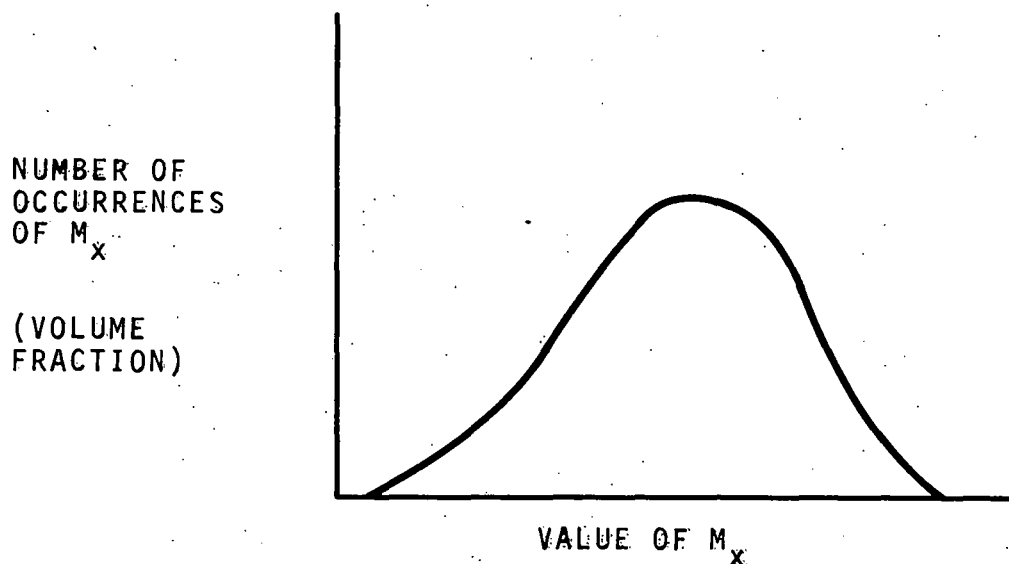
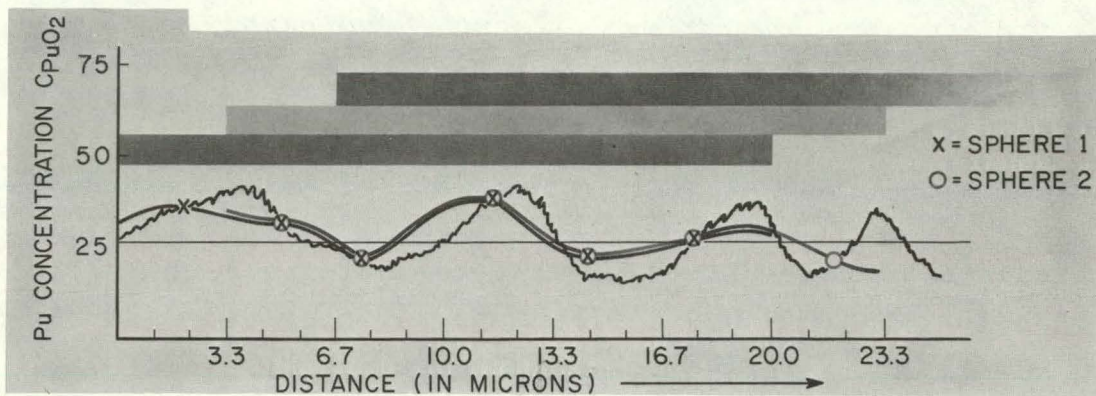


FIGURE 3. Hypothetical Distribution Curve for Figure of Merit M_x in a Heterogeneous UO_2 - PuO_2 Fuel Pellet

EXPERIMENTAL RESULTS OF MODEL

The microprobe data from three $(Pu_{0.25}U_{0.75})O_2$ fuel pellets with four different degrees of inhomogeneity were analyzed according to the homogeneity model given above. Pellet 1 was wet ballmilled \sim 16 hours, Pellet 2 was a typical

irradiation test pellet used in PNL-3 fuel pins, dry ballmilled ~40 hours, Pellet 3 was dry ballmilled ~20 hours. Pellet 4 was dry ballmilled ~10 hours. The microprobe traces were analyzed for the average PuO_2 content (\bar{C}_{PuO_2}) along 20 micron increments centered at 3.3 micron intervals, and the actual PuO_2 content (C_{PuO_2X}) at the center of each 20 micron increment (Figure 4).



$$\bar{C}_{\text{PuO}_2} X(\text{SPHERE 1})_{0 \mu \text{ TO } 20 \mu} = \left[\bar{C}_{\text{PuO}_2} \Big|_{0}^{3.3} + \bar{C}_{\text{PuO}_2} \Big|_{3.3}^{6.7} + \bar{C}_{\text{PuO}_2} \Big|_{6.7}^{10.0} + \bar{C}_{\text{PuO}_2} \Big|_{10.0}^{13.3} \right. \\ \left. + \bar{C}_{\text{PuO}_2} \Big|_{13.3}^{16.7} + \bar{C}_{\text{PuO}_2} \Big|_{16.7}^{20.0} \right] / 6$$

$$\bar{C}_{\text{PuO}_2} X(\text{SPHERE 1}) = \text{CONCENTRATION } \text{PuO}_2 \text{ WHERE } X = 10 \text{ (SPHERE 1)}$$

$$\bar{C}_{\text{PuO}_2} O(\text{SPHERE 2}) = \left[\bar{C}_{\text{PuO}_2} \Big|_{3.3}^{6.7} + \bar{C}_{\text{PuO}_2} \Big|_{6.7}^{10.0} + \bar{C}_{\text{PuO}_2} \Big|_{10.0}^{13.3} + \bar{C}_{\text{PuO}_2} \Big|_{13.3}^{16.7} \right. \\ \left. + \bar{C}_{\text{PuO}_2} \Big|_{16.7}^{20.0} + \bar{C}_{\text{PuO}_2} \Big|_{20.0}^{23.3} \right] / 6$$

$$\bar{C}_{\text{PuO}_2} O(\text{SPHERE 2}) = \text{CONCENTRATION } \text{PuO}_2 \text{ WHERE } X = 13.3 \text{ (SPHERE 2)}$$

FIGURE 4. Plutonium Concentration for Theoretic 20 Micron Sphere

The pellets were identified as 4, 3, 2 and 1, and ranged from least homogeneous to most homogeneous, respectively. Alpha-autoradiographs of these pellets are shown in Figure 5. Analyses of the microprobe traces yielded the following data for each pellet.

Pellet Identification	\bar{M}	$\sigma_{\bar{M}}$
1	1.0000	0.01726
2	0.9962	0.06404
3	0.9877	0.12986
4	0.96645	0.19295

Results of the test thus indicate that the four pellets were greater than $\bar{M} = 0.95$. The model also proved that the homogeneity specification could be opened up by use of the figure of merit technique. The M_x frequency distribution histograms for each pellet are shown in Figure 6, 7, 8, and 9.

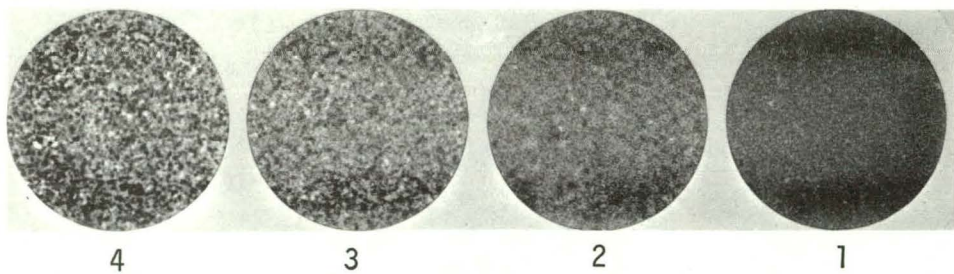


FIGURE 5. Homogeneity Results

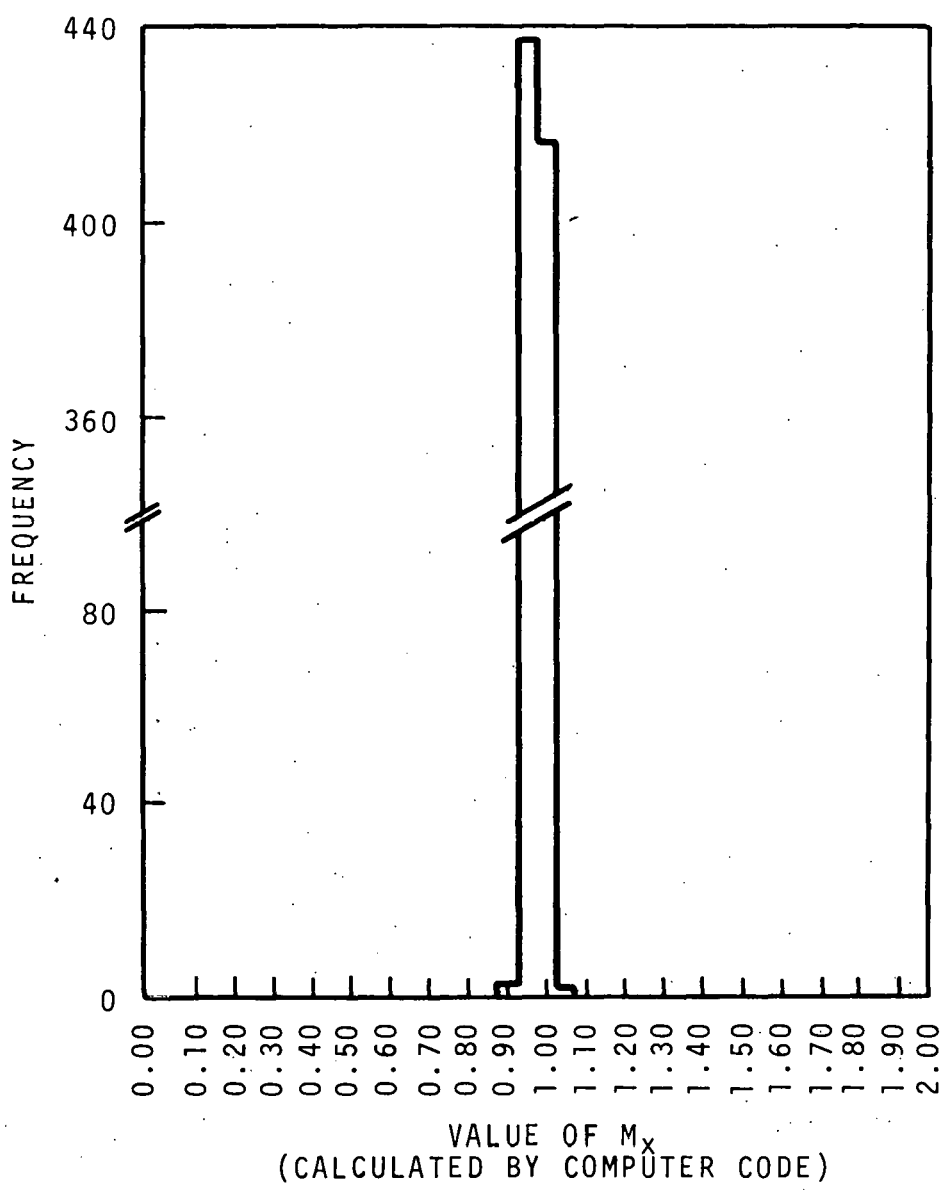


FIGURE 6. Figure of Merit Distribution
for Pellet 1

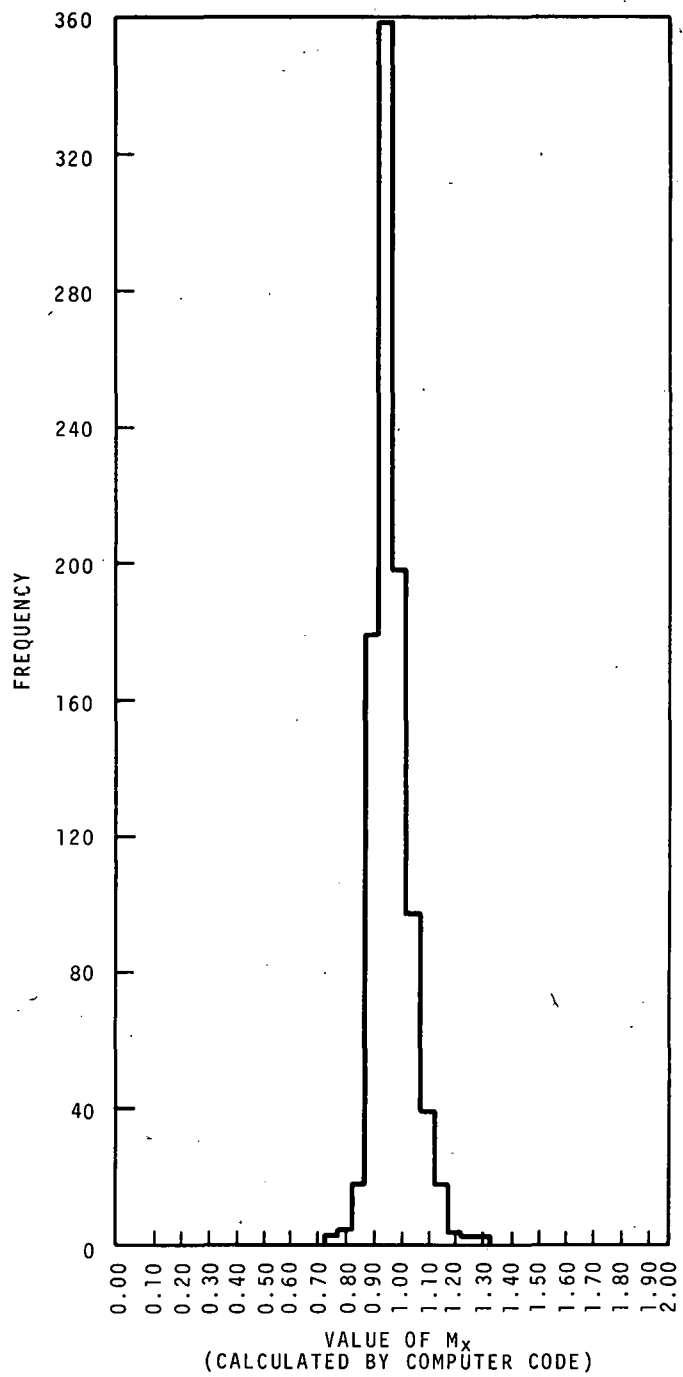


FIGURE 7. Figure of Merit Distribution for Pellet 2

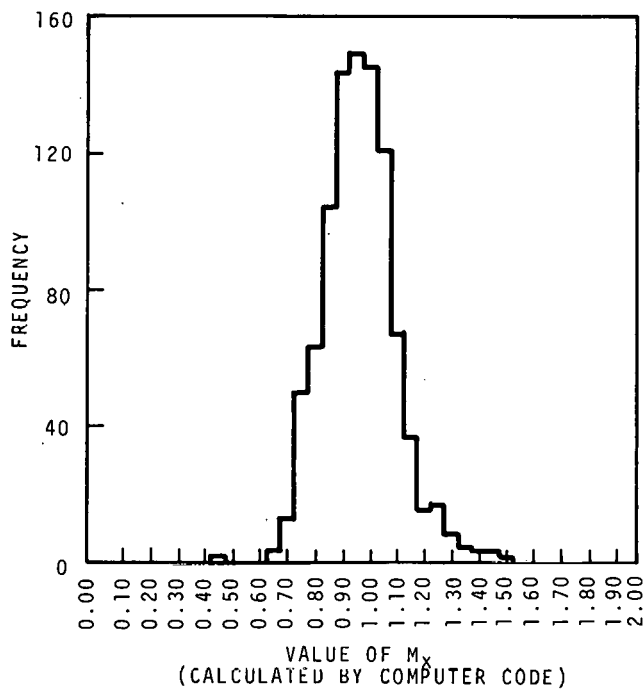


FIGURE 8. Figure of Merit Distribution for Pellet 3

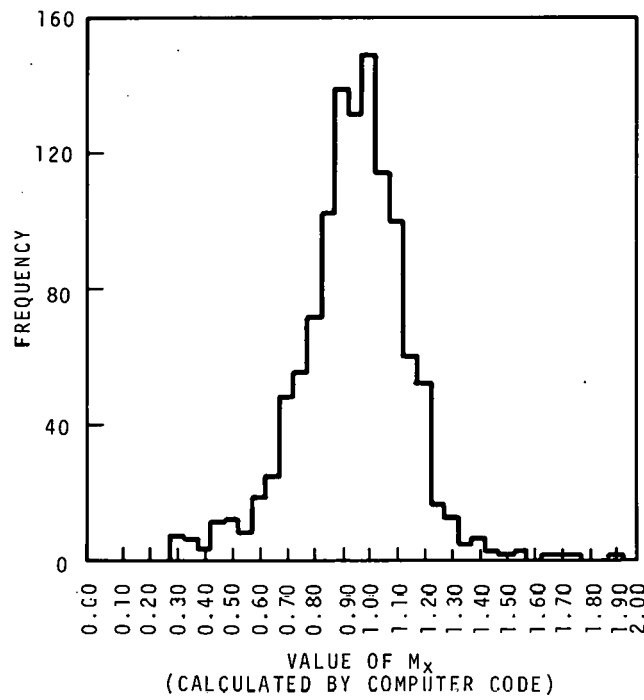


FIGURE 9. Figure of Merit Distribution for Pellet 4

APPLICATION OF HOMOGENEITY MODEL

A computer code was written to calculate the figure of merit of fuel pellets. The code converts the data from the microprobe punch tape into the computer program and calculates the figure of merit. The computer code and the explanations as to the specific functions of the statements in the computer code are given in the Appendix.

In order for industry to use this figure of merit model to establish homogeneity in the reactor fuel, it was determined that the correlation between figure of merit and alpha-autoradiography would be developed. This would permit the utilization of a relatively inexpensive and simple test method. Standards were made having a range of figures of merit which were then alpha-autoradiographed. These standards of known homogeneity are compared to pellets with unknown homogeneity by using alpha-autoradiographs taken at the same time. From this visual comparison with the standards, a figure of merit for the unknown pellets can be determined (see Figure 10). This method of relating the figure of merit to alpha-autoradiography makes the homogeneity specification feasible for industrial measurement and use.

CONCLUSIONS

1. Quantitative characterization of a UO_2 - PuO_2 fuel pellet matrix can be accomplished by scanning pellets with an electron microprobe for PuO_2 concentration sizes of PuO_2 enriched or depleted zones, and separation distance of such zones. Statistical analyses of the data indicated less than 1 percent probability of occurrence of zones with peak PuO_2 concentration greater than 50 wt%, and less than 1 percent probability of occurrence of PuO_2 enriched or depleted zones having diameters greater than 50 microns.

(FIGURES OF MERIT DETERMINED FROM ELECTRON MICROPROBE
ANALYSIS, ALL ALPHA-AUTORADIOGRAPHS ENLARGED TO 30X)

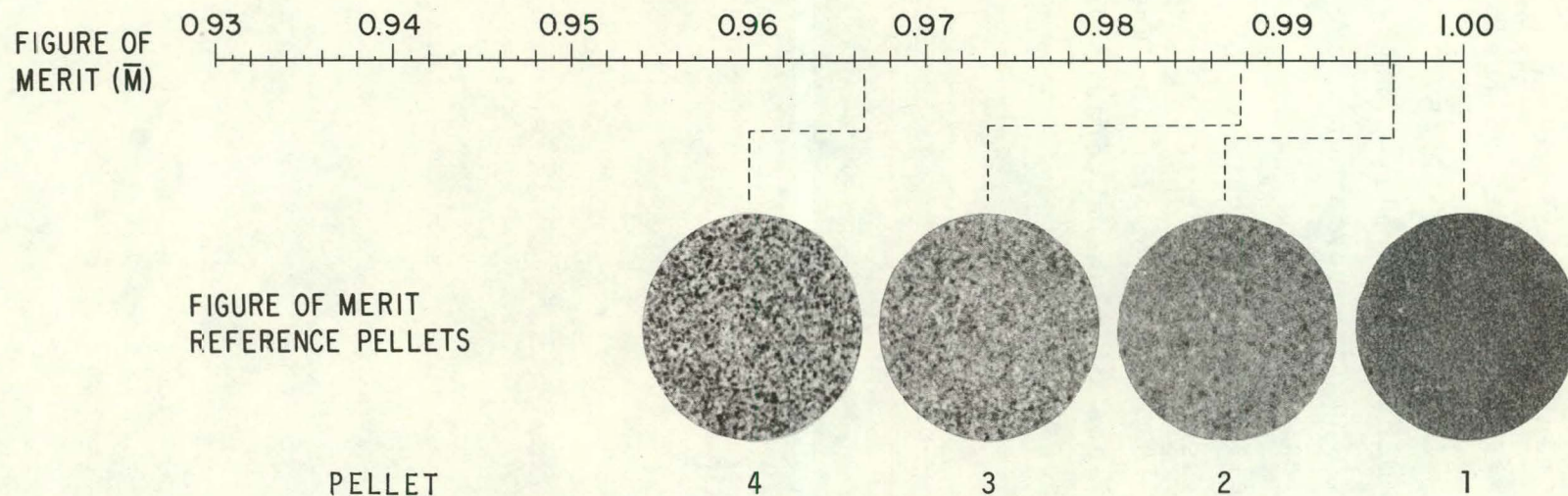


FIGURE 10. Determination of Fuel Pellet Homogeneity Using Figure of Merit Reference Pellets

2. The figure of merit mathematical model is a very good quantitative way to determine the fuel pellet homogeneity using the scanning electron microprobe.
3. The figure of merit model relates the fuel pellet homogeneity to the function performance of in-reactor energy deposition rates.
4. A feasible, relatively inexpensive and simple test method can be used for industrial measurement of fuel homogeneity. This consists of using known standards and visual comparisons of alpha-autoradiographs of unknown pellets and the standards.

ACKNOWLEDGMENTS

The authors wish to acknowledge the efforts of B. Y. Katayama and R. D. Nelson for performing the micro-probe work. The mathematics model of the three dimensional graph is largely due to the efforts of R. L. Buschbom.

The development and debugging of the computer code were achieved under the leadership of R. L. Buschbom and J. D. Robinson.

Making the standards and coordinating the running of the standards to obtain the figures of merit are due to the efforts of T. E. Stallwood and J. D. Robinson.

REFERENCES

1. E. R. Astley. Fast Flux Test Facility Quarterly Technical Report September, October, November 1969, BNWL-1275, Battelle-Northwest, Richland, Washington.
2. Dr. Herman S. Rosenbaum, General Electric Company, Vallecitos Nuclear Center. "Fuel Analysis Difficulties in U-Pu Standardization," Presented at the 1969 AEC Microprobe Users Conference, Pasadena, California.
3. RDT Standard E13-6, FFTF Driver Fuel Pin Fuel Pellet.
4. R. E. Peterson. Neutron Kinetics Problems Associated with Mixed Oxide Fuels, HW-81259. Available from Clearinghouse for Federal Scientific and Technical Information, Springfield, Virginia, 1964.
5. W. W. Little, Jr. Unpublished Data, WADCO Corporation, January 19, 1968. (BNW internal memo to P. L. Hofmann, Effect of Fuel Grain Size on FTR Safety Characteristics.)

WHAN-FR-20

APPENDIX

BIT FR57* MAIN:MAIN
UNIVAC 1108 FORTRAN V LEVEL 220E 0009 F600A - CSC005.
THIS COMPIILATION WAS DONE ON 25 SEPT 70 AT 12:13:25

MAIN PROGRAM

STORAGE USED (BLOCK, NAME, LENGTH)

0001	*CODE	000010
0000	*DATA	000001
0002	*BLANK	000000

EXTERNAL REFERENCES (BLOCK, NAME)

0003	PTCNV
0004	PROBEZ
0005	EXIT
0006	STOP\$

STORAGE ASSIGNMENT FOR VARIABLES (BLOCK, TYPE, RELATIVE LOCATION, NAME)

1. 00101	CALL PTCNV
2. 00103	CALL PROBEZ
3. 00104	CALL EXIT
4. 00105	END

*NEW

END OF UNIVAC 1108 FORTRAN V COMPIILATION. **DIAGNOSTIC** MESSAGE(S)

PHASE 1 TIME = 0 SEC.
PHASE 2 TIME = 0 SEC.
PHASE 3 TIME = 0 SEC.
PHASE 4 TIME = 0 SEC.
PHASE 5 TIME = 0 SEC.
PHASE 6 TIME = 0 SEC.

TOTAL COMPIILATION TIME = 0 SEC

MAIN	SYMBOLIC	
MAIN	CODE	RELOCATABLE

14 NOV 69	04:50:46	0	00526206	28	3 (DELETED)
14 NOV 69	04:50:46	1	00526122	48	1 (DELETED)
0	00526152	28	2		

BIT FRS PROBE,PROBE
UNIVAC 1108 FORTRAN V LEVEL 2206 0009 F600A - CSC005
THIS COMPILATION WAS DONE ON 25 SEP 70 AT 12:13:26

ROUTINE PROBE ENTRY POINT 000502

PROBE2 ENTRY POINT 000534

STORAGE USED (BLOCK, NAME, LENGTH)

0001	*CODE	000537
0000	*DATA	004045
0002	*BLANK	000000
0003	UGH	003737
0004	CHIT	007641
0005	AUD	007640

EXTERNAL REFERENCES (BLOCK, NAME)

0006	OFFSET
0007	NRDUS
0010	N101\$
0011	N102\$
0012	NPRT\$
0013	NERR\$

STORAGE ASSIGNMENT FOR VARIABLES (BLOCK, TYPE, RELATIVE LOCATION, NAME)

0001	000122	10L	0000	004003	102F	0000	003747	11F	0000	003774	12F	0001	000034	142G	
0000	003743	2F	0001	000172	20L	0001	000376	250L	0001	000266	30L	0001	000044	300L	
0001	000012	30L	0000	003746	4F	0000	003735	AA	0000	003741	AAX	0004	000000	AX	
0005	R	000000	AXX	0000	R	003736	BB	0000	R	003740	BBX	0004	R	003720	BXX
0003	000000	DATA	0000	R	000000	F	0000	R	003742	FRAC	0004	R	007640	FRAC2	
0000	I	003722	I	0000	I	003727	IJ	0000	I	003734	I\$	0000	I	003721	J
0000	I	003725	LL	0000	I	003720	M	0000	I	003723	MM	0000	I	003726	MODE
0003	R	003721	QINC	0003	R	003720	SCALE	0000	R	003730	VA1	0000	R	003731	VA2
0000	R	003733	VB2	0003	R	003722	XNEG					0000	R	003732	VB1

① 00101 SUBROUTINE PROBE(A,B,C,D)
2. 00103 COMMON /UGH/ DATA(2000),SCALE,QINC,XNEG,HEAD(12)
3. 00104 COMMON /CHIT/ AX(2000),BX(2000),FRAC2

```

4. 00105      COMMON/ADD/AXX(2000), BXX(2000)
5. 00106      DIMENSION F(2000)
6. 00107      DATA M/0//J/0//I/0//MM/0//L/0//LL/0/
7. 00116      DATA MODE/0/,IJ/0/
8. 00121      2 FORMAT(4F10.0/12A6)
9. 00122      4 FORMAT()
10. 00123      11 FORMAT('1' 5X'SPECTROMETER 1' 9X'SPECTROMETER 2' 9X'PERCENT 002*10
11. 00123      *X'PERCENT PJO2*8X'NORMALIZED U02'7X'NORMALIZED PU02//)
12. 00124      12 FORMAT(5X;1PE23.4*10X;IPE13.4;4*(8X;IPE13.4))
13. 00125      1F (IJ,EQ.5) GO TO 301
14. 00127      IJ=IJ+1
15. 00130      RETURN
16. 00131      301 CONTINUE
17. 00132      1F (MODE,EQ.1) GO TO 300
18. 00134      READ(5,27) VA1*VA2*VB1*VB2,HEAD
19. 00146      PRINT 11,
20. 00150      300 MODE=1
21. 00151      1F (M.GT.10) GO TO 30
22. 00153      1F (M.EQ.10) GO TO 10
23. 00155      M=M+1
24. 00156      1F (A.LT.2..0R.C.LT.2.) RETURN
25. 00160      MM=MM+1
26. 00161      AA=AA+1.*A=(VA1*VA2*C)
27. 00162      RETURN
28. 00163      10 1F (L.EQ.1C) GO TO 20
29. 00165      L=L+1
30. 00166      1F (B.LT.2..0R.C.LT.2.) RETURN
31. 00170      LL=LL+1
32. 00171      BB=BB+1.*B=(VB1*VB2*C)
33. 00172      RETURN
34. 00173      20 AA=AA/MM
35. 00174      BB=BB/LL
36. 00175      M=11
37. 00176      30 1F (A.LT.2..0R.B.LT.2..0R.C.LT.2.) RETURN
38. 00200      1F (U.LT.400..0R.D.GE.500.) RETURN
39. 00202      I=I+1
40. 00203      BX(I)=100.*((1.*B-VB1-VB2*C)/BB
41. 00204      AX(I)=100.*((1.*A-VA1-VA2*C)/AA
42. 00205      F(I)=100.*((AX(I))+BX(I))
43. 00206      AXX(I)=AX(I) * F(I)
44. 00207      BXX(I)=BX(I) * F(I)
45. 00210      1F (BX(I).LT.0..0R.AX(I).LT.0.) GO TO 250
46. 00212      P=P+BXX(I)
47. 00213      PRINT 12, A,B,AX(I),BX(I),AXX(I),BXX(I)
48. 00223      BBX=BBX+BXX(I)
49. 00224      AX=AXX+AX(I)
50. 00225      RETURN
51. 00226      250 I=I-1
52. 00227      RETURN

```

```
53. 00230  ENTRY PROBE2
54. 00231  READ(5,2) SCALE,QINC,XNEG
55. 00236  FRAC=BBX/I
56. 00237  FRAC2=P/I
57. 00240  PRINT 102, FRAC,FRAC2
58. 00244  102  FORMAT(//5X,NON-NORMALIZED PU02 AVG.'1PE13.4.', NORMALIZED PU02
59. 00244  1  AVG.'1PE13.4')
60. 00245  FRAC2=FRAC2/100.
61. 00246  CALL OFFSET(I)
62. 00247  RETURN
63. 00250  END
```

END OF UNIVAC 1108 FORTRAN V COMPILATION. 0 *DIAGNOSTIC* MESSAGE(S)
PHASE 1 TIME = 0 SEC.
PHASE 2 TIME = 0 SEC.
PHASE 3 TIME = 0 SEC.
PHASE 4 TIME = 0 SEC.
PHASE 5 TIME = 0 SEC.
PHASE 6 TIME = 0 SEC.

TOTAL COMPILATION TIME = 1 SEC
PROBE SYMBOLIC
PROBE CODE RELOCATABLE

14 NOV 69 04:51:03	0	00531654	28	11 (DELETED)
14 NOV 69 04:51:03	1	00531446	72	1 (DELETED)
	0	00531512	28	7

A-4

WIT FR5 OFFSET,OFFSET
UNIVAC 1108 FORTRAN V LEVEL 2206 0009 F600A - CSC005
THIS COMPILED ON 25 SEP 70 AT 12:13:27

SUBROUTINE OFFSET ENTRY POINT 000125

STORAGE USED (BLOCK, NAME, LENGTH)

0001	*CODE	000145
0000	*DATA	003762
0002	*BLANK	000000
0003	UGH	003737
0004	CHIT	007641
0005	ADD	007640

EXTERNAL REFERENCES (BLOCK, NAME)

0006	HISTO
0007	NWDUS
0010	N102%
0011	N101%
0012	NERR3%

STORAGE ASSIGNMENT FOR VARIABLES (BLOCK, TYPE, RELATIVE LOCATION, NAME)

0001	000004	IIUG	0001	000016	115G	0001	000064	136G	0001	000076	144G	0000	003730	19F
0000	003735	30F	0004	000000	AX	0005	R 000000	AXX	0004	003720	BX	0005	R 003720	BXX
0000	R 000000	U	0003	R 000000	DATA	0000	R 003726	F	0004	R 0007640	FRAC2	0003	003723	HEAD
0000	I 003720	J	0000	I 003721	JK	0000	I 003727	X	0000	I 003723	L	0003	003721	QINC
0003	003720	SCALE	0003	003722	XNEG	0000	R 003725	XY	0000	R 003724	YX	0000	R 003722	Z

① 00101 SUBROUTINE OFSET(I)
2. 00103 COMMON /UGH/ DATA(2000),SCALE,QINC,XNEG,HEAD(12)
3. 00104 COMMON /CHIT/ AX(2000),BX(2000),FRAC2
4. 00105 COMMON /ADU/ AXA(2000),BXX(2000)
5. 00106 DIMENSION D(2000)
6. 00107 DO 10 J=1,1
7. 00112 JK=J-10
8. 00113 Z=U
9. 00114 DO 11 L=JK,J
10. 00117 Z=Z + BXX(L)

11. 00120 11 CONTINUE
12. 00122 Z=Z/1100.
13. 00123 YX=AXX(J-5)/100.
14. 00124 XY=8XX(J-5)/100.
15. 00125 D(JK)=(.026+.948*Z)*(1.-XY)
16. 00126 10 CONTINUE
17. 00130 F=(.026+.948*FRAC2)*(1.-FRAC2)
18. 00131 I=1-10
19. 00132 WRITE(6,19)
20. 00134 19 FORMAT(2I11, FIGURE OF MERIT, //)
21. 00135 DO 20 J=1,FY
22. 00140 20 DATA(J)=D(J)/F
23. 00142 20 WRITE(6,30), (DATA(K), K=1, I)
24. 00150 30 FORMAT(10(IPE13,4))
25. 00151 CALL HISTOT1
26. 00152 RETURN
27. 00153 END

END OF UNIVAC 1108 FORTRAN V COMPILATION. 0 *DIAGNOSTIC* MESSAGE(S)
PHASE 1 TIME = 0 SEC.
PHASE 2 TIME = 0 SEC.
PHASE 3 TIME = 0 SEC.
PHASE 4 TIME = 0 SEC.
PHASE 5 TIME = 0 SEC.
PHASE 6 TIME = 0 SEC.

TOTAL COMPILATION TIME = 1 SEC

WIT FRS HISTO,HISTO
UNIVAC 1108 FORTRAN V LEVEL 22C6 0009 F600A - CSC005
THIS COMPILED WAS DONE ON 25 SEP 70 AT 12:13:28

SUBROUTINE HISTO ENTRY POINT 000763

STORAGE USED (BLOCK, NAME, LENGTH)

0001	*CODE	001004
0000	*DATA	016326
0002	*BLANK	000000
0003	UGH	003737

EXTERNAL REFERENCES (BLOCK, NAME)

0004	NWDUS
0005	NI01\$
0006	NI02\$
0007	SQRT
0010	NPRT\$
0011	NERR3\$

STORAGE ASSIGNMENT FOR VARIABLES (BLOCK, TYPE, RELATIVE LOCATION, NAME)

0000	016163	1F	0000	016140	12F	0000	016145	13F	0000	016167	14F	0001	000017	1526	
0001	000026	156G	0000	016172	16F	0000	016173	18F	0000	016177	19F	0000	016105	2F	
0001	000122	204G	0001	000142	21L	0001	000132	216G	0001	000245	266G	0001	000253	274G	
0000	0161C7	3F	0001	000270	306G	0001	000274	314G	0001	000302	323G	0001	000321	337G	
0001	000357	352G	0001	000341	355G	0000	016111	4F	0001	000211	40L	0001	000405	410G	
0001	000416	417G	0001	000434	427G	0001	000175	43L	0001	000446	435G	0001	000205	44L	
0001	000560	472G	0000	016115	5F	0001	000730	500L	0001	000732	501L	0001	000567	502L	
0000	016221	503F	0000	016231	505F	0001	000701	506L	0001	000652	507L	0001	000313	51L	
0001	000650	515G	0000	016122	6F	0001	000332	61L	0000	016125	7F	0001	000452	70L	
0001	000401	75L	0001	000370	77L	0000	016130	8F	0000	016135	9F	0000	R	016062	AVE
0000	R	016014	CONF	0000	R	016102	CONIN1	0000	R	016101	CONIN2	0003	R	000000	DATA
0003	R	003723	HEAD	0000	R	015530	HIST	0000	I	016043	I	0000	I	007640	IFR
0000	I	016051	INC	0000	I	015674	ITEST	0000	I	016046	I\$	0000	I	016066	J
0000	I	016060	K	0000	I	000000	KFR	0000	I	016056	KKK	0000	I	016045	KVAR
0000	I	016072	LL	0000	I	016073	LLL	0000	I	016052	MM	0000	I	016026	MEGF
0000	I	016055	NX	0000	R	016067	PINC	0003	R	003721	QINC	0003	R	003720	SCALE
0000	R	016063	SOS	0000	R	016054	SSX	0000	R	016053	SX	0000	R	016040	SYM1
0000	R	016042	SYM3	0000	R	016074	TERP	0000	R	016075	TOL	0000	R	016076	TOL1
0000	R	016064	VAR	0000	R	016057	X	0000	R	016050	XINC	0000	R	016061	XN
0000	R	016047	XNN	0000	R	003720	ZINC					0003	R	003722	XNEG

```

1. 00101 1 SUBROUTINE HISTO (N)
2. 00103 1 FORMAT(1H1,12A6)
3. 00104 2 FORMAT (3F10.0)
4. 00105 3 FORMAT (F11.0)
5. 00106 4 FORMAT (18X,1H.,100A1,1H.)
6. 00107 5 FORMAT (1X,F10.3,15,3H ..,100A1,1H.)
7. 00110 6 FORMAT (18X,IU2(1H,1))
8. 00111 7 FORMAT (1X,119(1H*)//)
9. 00112 8 FORMAT (1X,F10.3,7X,1H..,100X,1H..)
10. 00113 9 FORMAT (18X,1H.,100X,1H.)
11. 00114 12 FORMAT (///////11HIEND OF JOB)
12. 00115 13 FORMAT (////18X, 1HN,7X,3HSUM,9X,10HSUM OF, SQ.,8X,4HMEAN,
13. 00115 16X,14HSUM OF DEV:SQ,75X,8HVARIANC,3X,15H STD:DEV.)
14. 00116 14 FORMAT (9X, I10,1P6E15.6)
15. 00117 16 FORMAT (214)
16. 00120 18 FORMAT (1H*,6H INC =,F9.3)
17. 00121 19 FORMAT (/////IX,157-88H OBSERVATIONS WERE INCLUDED IN THE ABOVE SU
18. 00121 MMARY, BUT WERE OUT OF RANGE OF THE HISTOGRAM)
19. 00121 C
20. 00122 COMMON /UGH/ DATA(2000),SCALE,QINC,XNEG,HEAD(12)
21. 00123 DIMENSION KFR(2000),ZINC(2000)
22. 00124 DIMENSION IFR(3000),HIST(100)
23. 00125 DIMENSION ITEST(40),FACT(40),CONF(10),NEGF(10)
24. 00126 DATA SYM1/0050505050505/
25. 00130 DATA SYM2/6HX /
26. 00132 DATA SYM3/0450505050505/
27. 00134 DATA (ITEST(I),I=1,35)/30,35,40,45,50,55,60,65,70,75,80,85,90,95,1
28. 00134 *00,110,120,130,140,150,160,170,180,190,200,250,300,400,500,600,700
29. 00134 *800,900,1000,5000/
30. 00136 DATA (FACT(I),I=1,35)/3.350,3.272,3.213,3.165,3.126,3.094,3.066,3.
31. 00136 *042,3.021,3.002,2.986,2.971,2.958,2.945,2.934,2.915,2.898,2.883,2.
32. 00136 *870,2.859,2.848,2.839,2.831,2.823,2.816,2.788,2.767,2.739,2.721,2.
33. 00136 *707,2.697,2.688,2.682,2.676,2.576/
34. 00140 DATA (CONF(I),I=1,9)/1.990,1.987,1.984,1.972,1.968,1.966,1.965,1.9
35. 00140 *621,959/
36. 00142 DATA (NEGF(I),I=1,9)/80,90,100,200,300,400,500,1000,5000/
37. 00142 C
38. 00144 IF (N)501,501,15
39. 00147 15 CONTINUE
40. 00150 NVAR=1
41. 00151 DO 500 KVAR=1,NVAR
42. 00151 C
43. 00154 WRITE (6,1) HEAD
44. 00162 WRITE (6,7)
45. 00164 XNN=SCALE

```

46. 00165 XINC=1.0/XNN
47. 00166 INC=(QINC*XNN)+0.5
48. 00167 MM=IU007/INC
49. 00170 WRITE (6,6)
50. 00172 WRITE (6718) QINC
51. 00175 WRITE (6,9)
52. 00177 WRITE (6,9)
53. 00201 WRITE (6,9)
54. 00201 C
55. 00203 DO 101=1,1000
56. 00206 IFR(I)=0
57. 00207 10 CONTINUE
58. 00207 C
59. 00211 SX=0.0
60. 00212 SSX=0.0
61. 00213 NX=0
62. 00214 KKK=0
63. 00214 C
64. 00214 C
65. 00215 DO 40 I=1,N
66. 00220 X=UATAT(I)
67. 00221 IF(X) 21,20,21
68. 00224 20 CONTINUE
69. 00225 IF(X.LT.0.0) GO TO 40
70. 00227 21 CONTINUE
71. 00230 SX=SX+X
72. 00231 SSX=SSX+X**2
73. 00232 NX=NX+1
74. 00233 X=X+XNEG
75. 00234 K=(X*XNN)
76. 00235 K=K+1
77. 00235 C
78. 00236 IF (K) 42,42,43
79. 00241 42 CONTINUE
80. 00242 KKK=KKK+1
81. 00243 43 CONTINUE
82. 00244 IF (K=1000) 44,44,45
83. 00247 45 CONTINUE
84. 00250 KKK=KKK+1
85. 00251 GO TO 40
86. 00252 44 CONTINUE
87. 00252 C
88. 00253 IFR(K)=IFR(K)+1
89. 00253 C
90. 00254 40 CONTINUE
91. 00254 C
92. 00254 C
93. 00256 XN=NX
94. 00257 AVE=SX/XN

```

91. 00260      SDS=(XN*SSX-SX**2)/XN
92. 00261      VAR=SDS/(XN-1.0)
93. 00262      SD=SORT(VAR)
94. 00262      C
95. 00263      J=0
96. 00264      PINC=-XNEG-QINC
97. 00265      DO 35 I=1,MM,L
98. 00270      KFR(I)=0
99. 00271      PINC=PINC+QINC
100. 00272      ZINC(I)=0.0
101. 00273      DO 34 J=I,INC
102. 00276      J=J+1
103. 00277      KFR(I)=KFR(I)+IFR(J)
104. 00300      34 CONTINUE
105. 00302      ZINC(I)=PINC
106. 00303      35 CONTINUE
107. 00303      C
108. 00305      DO 37 I=1,1000
109. 00310      IFR(I)=0
110. 00311      37 CONTINUE
111. 00311      C
112. 00313      DO 36 I=1,MM
113. 00310      IFR(I)=0
114. 00311      37 CONTINUE
115. 00311      C
116. 00313      DO 36 I=1,MM
117. 00316      IFR(I)=KFR(I)
118. 00317      36 CONTINUE
119. 00317      C
120. 00317      C
121. 00321      L=0
122. 00322      DO 50 I=1,1000
123. 00325      L=L+1
124. 00326      IF .(IFR(L))51,50,51
125. 00331      50 CONTINUE
126. 00333      51 CONTINUE
127. 00333      C
128. 00334      LL=L
129. 00334      C
130. 00335      L=1001
131. 00336      DO 60 I=1,1000
132. 00341      L=L-1
133. 00342      IF .(IFR(L))61,60,61
134. 00345      60 CONTINUE
135. 00347      61 CONTINUE
136. 00350      LLL=L
137. 00350      C
138. 00351      DO 70 I=LL,LLL
139. 00354      DO 71 J=1,160
140. 00357      HIST(J)=SYM1
141. 00360      71 CONTINUE
142. 00360      C
143. 00362      IF .(IFR(I)) 77,78,77

```

```

144. 00365 78 CONTINUE
145. 00366 WRITE (6,9)
146. 00370 WRITE (6,8) 2INC(I)
147. 00373 WRITE (6,9)
148. 00375 GO TO 70
149. 00376 77 CONTINUE
150. 00376 C
151. 00377 JJ=IFR(I)
152. 00400 IF (JJ=100)75,75,76
153. 00403 76 CONTINUE
154. 00404 JJ=99
155. 00405 HIST(100)=SYM3
156. 00406 75 CONTINUE
157. 00407 DO 72 J$1,JJ
158. 00412 HIST(J)$SYM2
159. 00413 72 CONTINUE
160. 00413 C
161. 00415 WRITE (6,4) (HIST(J),J=1,100)
162. 00423 WRITE (6,9) 2INC(I),IFR(I),(HIST(J),J=1,100)
163. 00433 WRITE (6,4) (HIS(J),J=1,100)
164. 00441 70 CONTINUE
165. 00441 C
166. 00443 WRITE (6,9)
167. 00445 WRITE (6,9)
168. 00447 WRITE (6,9)
169. 00451 WRITE (6,6)
170. 00453 WRITE (6,13)
171. 00455 WRITE (6,7)
172. 00457 WRITE (6,14) NX,SX,SSX,AVE,SDS,VAR,SD
173. 00470 J=0
174. 00471 DO 498 I=2,35
175. 00474 J=J+1
176. 00475 IF (NX.GE.1TEST(I-1).AND.NX.LT.1TEST(I)) GO TO 502
177. 00477 4,8 CONTINUE
178. 00501 5,2 CONTINUE
179. 00502 TERP=(NX-1TEST(J))/(1TEST(J+1)-1TEST(J))=(FACT(J)-FACT(J+1))
180. 00503 TOL=(FACT(J)-TERP)*SD
181. 00504 TOL1=AVE-TOL
182. 00505 TOL2=AVE+TOL
183. 00506 PRINT 503, TOL1,TOL2
184. 00512 5,3 FORMAT(//75X'TOLERANCE INTERVAL',/5X'PROBABILITY IS 0.95 THAT AT')
185. 00512 *LEAST 0.99 OF THE DISTRIBUTION WILL BE INCLUDED BETWEEN F10.3, AN
186. 00512 *D*F10.3)
187. 00513 IJK=1
188. 00514 DO 506 I=2,9
189. 00517 IF (NX.GE.NEGF(I-1).AND.NX.LT.NEGF(I)) GO TO 507
190. 00521 GO TO 506
191. 00522 5,7 CONIN2=AVE-CONF(IJK)*(SD/SQRT(NX))
192. 00523 CONIN1=AVE-CONF(IJK)*(SD/SQRT(NX))

```

```
193. 00524 506 IJK=IJK+1
194. 00526 PRINT 505, CONIN1,CONIN2
195. 00532 505 FORMAT(//,5X,CONFIDENCE INTERVAL//,5X,PROBABILITY IS 0.95 THAT THE
196. 00532 * POPULATION MEAN WILL BE INCLUDED BETWEEN F10.3, AND F10.3)
197. 00532 C
198. 00533 IF (KK<500,500,499
199. 00536 499 CONTINUE
200. 00537 WRITE (6,19) KKK
201. 00537 C
202. 00542 500 CONTINUE
203. 00544 501 CONTINUE
204. 00545 WRITE (6,12)
205. 00547 RETURN
206. 00550 END
```

END OF UNIVAC 1108 FORTRAN V COMPILATION. 0 *DIAGNOSTIC* MESSAGE(S)

PHASE 1 TIME = 1 SEC.
PHASE 2 TIME = 0 SEC.
PHASE 3 TIME = 0 SEC.
PHASE 4 TIME = 0 SEC.
PHASE 5 TIME = 0 SEC.
PHASE 6 TIME = 1 SEC.

TOTAL COMPILATION TIME = 2 SEC

The following is a list of explanations as to the specific functions of statements in the computer code used to calculate the figure of merit. The numbers associated with the explanations are the numbers circled in the preceding listing of computer code subroutines.

1. Subroutine Probe (A,B,C,D)--Prepares raw data from electron microprobe for figure of merit calculation and determines average PuO_2 percentage along diameter of pellet.
18. Reads into code the coefficients for spectrometer background equations (VA1, VA2, VB1, VB2), reads in the nominal PuO_2 percentage of the pellet (PERC), and reads in the heading for the histogram output page.
24. Sorts out bad data points caused by improperly punched points on paper tape readout by placing limits on the spectrometer readings (A for Spectrometer 1-- UO_2 , B for Spectrometer 2-- PuO_2 , and C for Spectrometer 3--background).
26. Sums 10 spectrometer readings (minus background) from Spectrometer 1 for standard 100 percent UO_2 spheroids.
30. See 24
32. Sums 10 spectrometer readings (minus background) from Spectrometer 2 for standard 100 percent PuO_2 spheroids.
34. Averages standard UO_2 spectrometer readings to give an average reading for Spectrometer 1 which is equivalent to 100 percent UO_2 .

35. Averages standard PuO_2 spectrometer readings to give an average reading for Spectrometer 2 which is equivalent to 100 percent PuO_2 .
37. See 24
38. Sorts out bad data points, such as those caused by voids, by placing limits on the specimen current (indicated by D).
40. For PuO_2 percentage at each data point, subtracts background, ratios the background corrected PuO_2 spectrometer readings to the average reading for 100 percent PuO_2 and converts this decimal fraction to a percentage.
41. For UO_2 percentage at each data point, subtracts background, ratios the background corrected UO_2 spectrometer readings to the average reading for 100 percent UO_2 and converts this decimal fraction to a percentage.
42. For each data point (each pair of UO_2 and PuO_2 percentages), calculates a normalization factor which ratios the sum of the two relative percentages to 100 percent. This factor compensates for the inherent error ($\sim \pm 2$ percent) in the electron micro-probe readings.
43. Normalizes each UO_2 percentage [AXX(I)] and each PuO_2 percentage [BXX(I)] so that the sum at each data point equals 100 percent. This step is the final step in preparing data for use in the figure of merit calculation (in Subroutine Offset). The code uses these normalized values of PuO_2 percentage for the figure of merit calculations.
44. See 43

45. Sorts out bad data points (negative percentages) caused by the inherent error in electron microprobe readings.
46. Sums PuO_2 percentages after they have been normalized to 100 percent.
47. Prints out, for each good data point, the UO_2 spectrometer reading (not including the 100 percent UO_2 standard points), the PuO_2 spectrometer reading (not including the 100 percent PuO_2 standard points), the UO_2 percentage prior to normalization, the PuO_2 percentage prior to normalization, the UO_2 percentage following normalization, and the PuO_2 percentage following normalization.
48. Sums PuO_2 percentages prior to normalization.
49. Sums UO_2 percentages prior to normalization.
55. Averages PuO_2 percentages prior to normalization, giving an overall non-normalized percentage along a diameter of the fuel pellet.
56. Averages normalized PuO_2 percentages, giving an overall normalized percentage along a diameter of the fuel pellet.
57. Prints out the overall non-normalized PuO_2 percentage (FRAC or BBX/I) and the overall normalized PuO_2 percentage (FRAC2 or P/I).

1. Subroutine Offset (I) - Calculates local and overall average figures of merit using PuO_2 percentages supplied by Subroutine Probe.
10. Sums eleven normalized PuO_2 percentage values for eleven consecutive points along the diameter of a 20 micron sphere (at 2 micron intervals) on the fuel pellet.
12. Averages eleven PuO_2 percentages and converts average value to a decimal fraction.
14. Converts PuO_2 percentage at midpoint of 20 micron sphere (middle point of eleven) to a decimal fraction.
15. Calculates numerator of local figure of merit expression where Z is the average PuO_2 percentage along diameter of 20 micron sphere and XY is the PuO_2 percentage at the center of the sphere.
17. Calculates denominator of local figure of merit expression where PERC is the nominal PuO_2 percentage (25%) of the fuel pellet.
22. Calculates local figures of merit for each of a series of points located at 2 micron intervals along a diameter of the fuel pellet (number of local figures of merit will be ten less than the total number of data points examined along the pellet diameter).
23. Prints out a local figure of merit value for each location at 2 micron intervals along a diameter of the fuel pellet (number of local figures of merit will be ten less than the total number of data points examined along the pellet diameter).

1. Subroutine Histo(N)--Sets up histogram for local figure of merit values and calculates statistical characteristics of local figure of merit distribution (including the average figure of merit).
71. Adds all calculated local figures of merit.
72. Adds the squares of all calculated local figures of merit.
94. Calculates average of all local figures of merit, giving the mean figure of merit for the pellet.
95. Calculates the sum of the deviation squared.
96. Calculates the variance for the figure of merit distribution.
97. Calculates the standard deviation for the figure of merit distribution.
172. Prints out the number of local figures of merit calculated, the sum of the local figures of merit, the sum of the squares of the local figures of merit, the average of the local figures of merit, the sum of the deviation squared, the variance, and the standard deviation.
180. Calculates tolerance interval for the figures of merit.
181. Calculates the lower tolerance limit for the figures of merit.
182. Calculates the upper tolerance limit for the figures of merit.
183. Prints out the lower and upper tolerance limits for the local figures of merit.

191. Calculates the upper confidence limit for the figures of merit.
192. Calculates the lower confidence limit for the figures of merit.
194. Prints out the lower and upper confidence limits for the local figures of merit.

DISTRIBUTIONNo. of CopiesOFFSITE

1 AEC Chicago Patent Group
 G. H. Lee

210 AEC Division of Technical Information Extension

26 AEC Division of Reactor Development and Technology
 Director, RDT
 Asst Dir for Nuclear Safety
 Analysis & Evaluation Br, RDT:NS
 Asst Dir for Plant Engrg, RDT
 Facilities Br, RDT:PE
 Components Br, RDT:PE
 Instrumentation & Control Br, RDT:PE
 Liquid Metal Systems Br, RDT:PE
 Asst Dir for Program Analysis, RDT
 Asst Dir for Project Mgmt, RDT
 Liquid Metals Projects Br, RDT:PM
 G. J. Mishko
 FFT Project Manager, RDT:RE
 Asst Dir for Reactor Engrg, RDT
 Control Mechanisms Br, RDT:RE
 Core Design Br, RDT:RE (2)
 Fuel Engineering Br, RDT:RE
 Fuel Handling Br, RDT:RE
 Reactor Vessels Br, RDT:RE
 Coolant Chemistry Br, RDT:RT
 Fuel Recycle Br, RDT:RT
 Fuels & Materials Br, RDT:RT
 Reactor Physics Br, RDT:RT
 Special Technology Br, RDT:RT
 Asst Dir for Engrg Standards, RDT
 LMFBR Program Manager, RDT:PM

1 AEC Idaho Operations Office
 Nuclear Technology Division
 C. W. Bills, Director

1 AEC San Francisco Operations Office
 Director, Reactor Division

No. of Copies

5 AEC Site Representatives
Argonne National Laboratory-CH
Argonne National Laboratory-ID
Atomics International
General Electric Co.
Westinghouse Electric Co.

3 Argonne National Laboratory
R. A. Jaross
LMFBR Program Office
N. J. Swanson

1 Atomic Power Development Assoc.
Document Librarian

5 Atomics International
FFTF Program Office (5)

2 Babcock & Wilcox Co.
Atomic Energy Division
S. H. Esleek
G. B. Garton

10 Bechtel Corporation
J. J. Teachnor, Project Administrator, FFTF

1 Combustion Engineering
1000 MWe Follow-On Study
W. P. Staker Project Manager

1 Combustion Engineering
Mrs. Nell Holder, Librarian

4 General Electric Company
Advanced Products Operation
Karl Cohen

1 General Electric Company
Nucleonics Laboratory
Dr. H. W. Alter, Mgr.

2 Gulf General Atomic Inc.
General Atomic Div.
D. Coburn

1 Idaho Nuclear Corporation
J. A. Buckham

No. of Copies

1 Liquid Metal Information Center
R. W. Dickinson

2 Liquid Metal Information Center
A. E. Miller

1 Oak Ridge National Laboratory
W. O. Harms

1 Stanford University
Nuclear Division
Division of Mechanical Engrg
R. Sher

1 United Nuclear Corporation
Research and Engineering Center
R. F. DeAngelis

1 WADCO Representative
R. M. Fleischman

11 Westinghouse Electric Corporation
Atomic Power Division
Advanced Reactor
D. C. Spencer

1 Westinghouse Electric Corporation (PFDL)
Cheswick, Pennsylvania
John Denero

ONSITE

1 AEC Chicago Patent Group
R. K. Sharp (Richland)

2 AEC RDT Asst Dir for Pacific Northwest Program

1 AEC Richland Operations Office
J. M. Shivley

7 Battelle-Northwest
Technical Information (5)
Technical Publication (2)

1 Bechtel Corporation
W. A. Smith (Richland)

No. of
Copies79 WADCO Corp.

G. J. Alkire	F. J. Leitz
H. J. Anderson	W. B. McDonald
S. O. Arneson	J. S. McMahon
J. M. Atwood	J. M. Norris
R. E. Bardsley	R. E. Peterson
C. A. Burgess	H. G. Powers (10)
C. P. Cabell	B. G. Rieck
J. R. Carrell	W. E. Roake
J. C. Cochran	G. J. Rogers
G. S. Cochrane	W. F. Sheely
W. H. Esselman	D. A. Stranik (10)
E. A. Evans	C. D. Swanson
W. M. Gajewski	K. G. Toyoda
K. M. Harmon	L. D. Turner
E. N. Heck	E. T. Weber
P. L. Hofman	B. Wolfe
J. N. Judy	W. R. Wykoff
J. P. Keenan	WADCO Document Control (15)
G. A. Last (10)	WADCO Tech Pubs (703)